Inorganic Chemistry

Communication

pubs.acs.org/IC

Charge Ordering and Carrier Generation by Air Oxidation of a Nickel Complex with Selenium-Containing Extended-Tetrathiafulvalenedithiolate Ligands

Hiroyuki Yajima,[†] Biao Zhou,[†] Emiko Fujiwara,[‡] Akiko Kobayashi,*[,†] and Hayao Kobayashi*[,†]

[†]Department of Chemistry, College of Humanities and Sciences, Nihon University, Sakurajosui 3-25-40, Tokyo 156-8550, Japan

[‡]Research Centre for Spectrochemistry, Graduate School of Science, The University of Tokyo, Hongo, Tokyo 113-0033, Japan

Supporting Information

ABSTRACT: The structures and electrical properties of (^{n}Bu$_4$N)[Ni(dmstfdt)$_2$] (**1**), (^{n}Bu$_4$N)$_2$[Ni(dmstfdt)$_2$] (**2**), and (^{n}Bu$_4$N)$_3$[Ni(dmstfdt)$_2$]$_2$ (**3**), where dmstfdt = extended-tetrathiafulvalenedithiolate ligand, were examined. The fresh crystal of **1** was found to be a Mott insulator, but the crystal gradually became highly conducting because of air oxidation. Compound **3** exhibited a semiconducting charge-ordering state.

Coulomb interactions between π electrons produce a variety of charge-ordering (CO) states,[1] which bring about remarkable transport phenomena such as giant nonlinear resistance (or an organic thyrister effect).[2] Seo et al. have recently proposed a "fragment molecular orbital (fragment MO) picture" of frontier orbitals,[3] which facilitates theoretical analyses of new ordering possibilities such as intramolecular CO (ICO) and intramolecular antiferromagnetic spin ordering in molecular conductors consisting of elongated π molecules (Figure 1).[4] The frontier MOs of the single-component

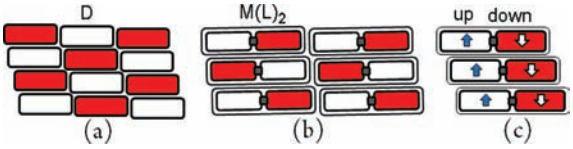

Figure 1. Schematic drawing of CO and spin-ordering structures. (a) Example of a CO structure in the conduction layer of π-donor molecules (D), where red and white squares represent the charge-rich and -poor molecules, respectively. (b) Example of a plausible ICO structure in a molecular conductor consisting of a transition-metal complex molecule with extended-TTF dithiolate ligands, M(L)$_2$. (c) Intramolecular antiferromagnetic spin ordering proposed for the antiferromagnetic metal [Au(tmdt)$_2$] (tmdt = trimethylenetetrathiafulvalenedithiolate).[4,6]

molecular metals [M(L)$_2$] were composed of two ligand π orbitals of extended-tetrathiafulvalenedithiolate (tetrathiafulvalene = TTF) ligands (L) and a d-like orbital localized around the central transition-metal atom (M).[3,5] By adopting an analogous "fragment MO picture", Tsuchiizu et al. recently reported the theoretical analysis of the possibility of ICO in a "half-filled organic metal", (TTM-TTP)I$_3$, which exhibits a metal−insulator transition at around 120 K; TTM-TTP {2,5-bis[4,5-bis(methylthio)-1,3-dithiol-2-ylidene]-1,3,4,6-tetrathiapentalene} is an elongated π-donor molecule.[7,8]

Herein, we examine the crystal structures of three nickel complexes of the selenium-containing extended-TTF dithiolate ligand dimethyldiselenadithiafulvalenedithiolate (dmstfdt; see Figure 2) with different oxidation states: (^{n}Bu$_4$N)[Ni(dmstfdt)$_2$] (**1**), (^{n}Bu$_4$N)$_2$[Ni(dmstfdt)$_2$] (**2**), and (^{n}Bu$_4$N)$_3$[Ni(dmstfdt)$_2$]$_2$ (**3**). The Ni(dmstfdt)$_2$ molecule, which consists of two extended-TTF dithiolate ligands connected by a Ni atom, is considered to be a suitable molecule for examining the possibility of ICO. In addition, we aimed to clarify the origin of the previously reported "weakly metallic behavior" of **1** around room temperature because the metallic properties of **1** with 1:1 stoichiometry appeared to be hardly understandable within the traditional concept on the electric properties of the molecular conductor.[9]

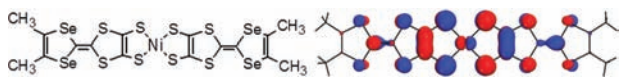

Figure 2. Line drawing of the Ni(dmstfdt)$_2$ molecule and illustration of the LUMO.[11]

Crystals of **1**−**3** were synthesized according to literature methods.[5a,9] X-ray diffraction experiments were performed using Rigaku Saturn 724R CCD and Mercury CCD systems.[10]

We have previously reported the crystal structure and electromagnetic properties of **1**.[9] However the X-ray crystal structure was reexamined in order to obtain more accurate bond lengths. The crystal structure of **1** contains two crystallographically independent molecules [labeled **A**(**1**) and **B**(**1**) in Table 1]. Because the average charge of Ni(dmstfdt)$_2$ in **1** is 1−, the lowest unoccupied MO (LUMO) of the neutral Ni(dmstfdt)$_2$ will be singly occupied (Figure 2). However, in the event that ICO is realized (see Figure 1b), localization of the excess charge causes the bond lengths of the lower half of the molecule ($a_l \sim g_l$) in Table 1 to become different from those of the upper half ($a_u \sim g_u$ in Table 1). Roughly speaking, if the excess charge tends to be localized on the lower half of the molecule, then the a_l, b_l, d_l, e_l, and g_l bonds will become longer and bonds c_l and f_l will become shorter than the corresponding bonds of the upper half of the molecule because

Received: December 13, 2011
Published: February 17, 2012

   dx.doi.org/10.1021/ic2026768 | *Inorg. Chem.* 2012, 51, 2731−2733

Table 1. Bond Lengths (Å) of Ni(dmstfdt)$_2^{n-}$ Anions[a]

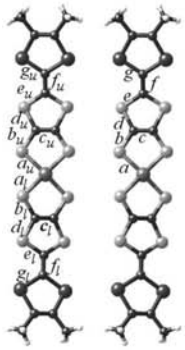

Mol.(Compd.)	$a_u(a)$	$b_u(b)$	$c_u(c)$	$d_u(d)$	$e_u(e)$	$f_u(f)$	$g_u(g)$	a_l	b_l	c_l	d_l	e_l	f_l	g_l
A(1)	2.170_2	1.717_5	1.357_8	1.760_5	1.762_6	1.352_7	1.888_6	2.166_2	1.710_6	1.374_8	1.750_6	1.761_6	1.326_7	1.898_7
B(1)	2.168_2	1.728_6	1.349_8	1.750_5	1.767_7	1.330_7	1.890_6	2.163_2	1.716_6	1.358_8	1.752_6	1.759_7	1.342_7	1.889_7
C(1)	2.167_2	1.718_6	1.360_8	1.753_5	1.762_7	1.338_7	1.892_6	.. Ni(dmstfdt)$_2^-$ (average bond length of **A(1)** and **B(1)**)						
D(2)	2.204_1	1.732_3	1.348_5	1.768_3	1.762_3	1.320_5	1.904_3	... Ni(dmstfdt)$_2^{2-}$						
I(3)	2.168_1	1.720_3	1.358_5	1.758_3	1.765_3	1.337_5	1.898_3	2.172_1	1.714_3	1.379_5	1.748_3	1.761_3	1.352_4	1.889_3
II(3)	2.167_1	1.719_3	1.366_4	1.760_3	1.763_3	1.345_5	1.897_3	2.170_1	1.710_3	1.367_4	1.753_3	1.768_3	1.336_5	1.899_3
III(3)	2.203_1	1.732_3	1.350_5	1.774_3	1.756_3	1.352_5	1.901_3	2.195_1	1.738_3	1.327_5	1.778_3	1.762_3	1.343_5	1.893_3
IV(3)	2.197_1	1.733_3	1.369_5	1.768_3	1.762_3	1.357_4	1.892_3	2.209_1	1.735_3	1.347_4	1.774_3	1.759_3	1.333_5	1.903_3

[a]The standard deviation of each bond length is given as a subscript. **A(1)** and **B(1)** are the average bond lengths of the two crystallographically independent molecules in **1**, obtained by assuming C_s symmetry of the ligands. **C(1)** represents bond lengths of the monoanionic molecule obtained by averaging $a_r \sim g_r$ and $a_l \sim g_l$ of **A(1)** and **B(1)**. **D(2)** is the average bond length of the dianionic molecule in **2**. **I(3)**–**IV(3)** are the average bond lengths of four crystallographically independent molecules in **3** (see Figure 4) obtained by assuming C_s symmetry of the ligands.

the excess electron will occupy the orbital that resembles the left-half (or right-half) of the LUMO with antibonding nature in the Ni–S and C–S(Se) bonds and bonding nature in the C=C bonds (see Figure 2). However, as seen from Table 1, no systematic difference in the values of $a_l \sim g_l$ and $a_u \sim g_u$ was observed for either of the molecules **A(1)** and **B(1)**; thus, the possibility of ICO in **1** was ruled out. In other words, the excess electron in Ni(dmstfdt)$_2^-$ tends to be equally distributed over both sides of the molecule.

Previously, we observed "weakly metallic behavior" of **1** at around room temperature despite the fact that the room-temperature conductivity was unusually small for a metallic conductor ($\sigma_{RT} \approx 0.2$ S cm^{-1}).[9] In order to clarify the origin of this curious resistivity behavior, four-probe resistivity measurements were performed repeatedly on many crystals. In contrast to the previous observation, the fresh crystals were found to be insulating ($\rho_{RT} \approx 10^4$ Ω cm), which is quite natural in view of the 1:1 stoichiometry and the results of above-mentioned X-ray structure analysis of **1**. That is, the fresh crystal of **1** is considered to be a Mott insulator. To clarify the origin of the previously observed weakly metallic behavior, repetitive measurements of the resistivity of **1** were taken over time, and it was found that the resistivity was significantly decreased by long-term exposure of the crystal to air; the color of the crystal changed from dark brown to black. The effect of exposure to air over time on the room-temperature resistivity, shown in Figure 3a, indicates a resistivity decrease of 3–4 orders of magnitude after 50 days, and the crystal exhibited an insulating transition at around 150 K (Figure 3b), as was previously observed.[9] To the best of our knowledge, such a large resistivity decrease by air oxidation has never been realized in the Mott insulating molecular crystal with a moderate room-temperature resistivity of about 10^4 Ω cm. The low room-temperature conductivity of the "aged crystal" clearly indicates that the crystal became highly conducting as a consequence of "carrier generation" due to air oxidation. The large room-temperature resistivity and the resistivity jump at 150 K observed even in the crystal whose storage time was only 15 days (A in Figure 3b) clearly indicated that the highly conducting region was gradually increased by the progress of oxidation. X-ray experiments were performed on the aged crystal. To our surprise, the diffraction patterns and the lattice constants were found to be approximately the same as those of the fresh crystal. Thus, **1** was found to be a very rare molecular crystal whose surface can be easily changed from the Mott insulating state to the highly conducting state by air oxidation.

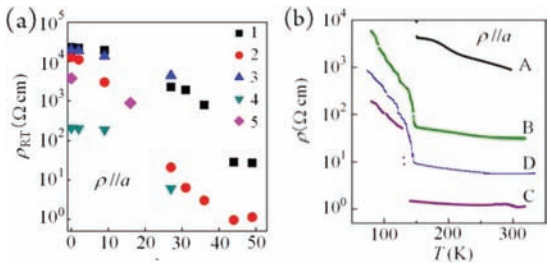

Figure 3. (a) Dependences of the room-temperature resistivity of four crystals (1–4) of **1** on the storage time (days) in air. (b) Temperature dependence of the resistivity of **1**: (A) crystal 4, after 15 days; (B) crystal 1, after 50 days; (C) crystal 2, after 50 days; (D) previously reported resistivity data.[9]

X-ray crystal structural analysis of **2** showed that the unit cell contains one crystallographically independent Ni(dmstfdt)$_2^{2-}$ unit. The bond lengths of the molecule are presented [**D(2)** in Table 1]. As expected from the bonding character of the LUMO (Figure 2), the Ni–S and C–S(Se) bonds of **D(2)** were found to be longer than those of the monoanion molecule **C(1)** (with the exception of bond *e*), and the C=C bonds of **D(2)** are shorter than those of **C(1)**. Because the resistivity of **2** (fresh crystal) was very high ($\rho_{RT} > 10^5$ Ω cm), no further resistivity measurements were performed.

The 3:2 stoichiometry of **3** suggested the possibility of metallic (or highly conducting) properties of the crystal. However, the resistivity measurements showed the crystal to be a semiconductor ($\rho_{RT} \approx 10^3$ Ω cm; $E_a \approx 0.018$ eV). Similar to **1**, the resistivity of **3** was decreased by long-term exposure of the crystal to air ($\rho_{RT} \approx 1.4 \times 10^2$ Ω cm; $E_a \approx 0.024$ eV after 60 days).

X-ray crystal structure analysis of **3** showed that the crystal belongs to the orthorhombic system and the unit cell contains 48 ^{n}Bu$_4$N$^+$ cations and 32 (or 4 crystallographically independent) Ni(dmstfdt)$_2$ anions. Ni(dmstfdt)$_2$ molecules are arranged to form two-dimensional layers parallel to the *ac* plane (see Figure 4). The unit cell contains four Ni(dmstfdt)$_2$ layers. Layers of ^{n}Bu$_4$N$^+$ cations are intercalated between the Ni(dmstfdt)$_2$ layers. The average bond lengths of the four

dx.doi.org/10.1021/ic2026768 | Inorg. Chem. 2012, 51, 2731–2733

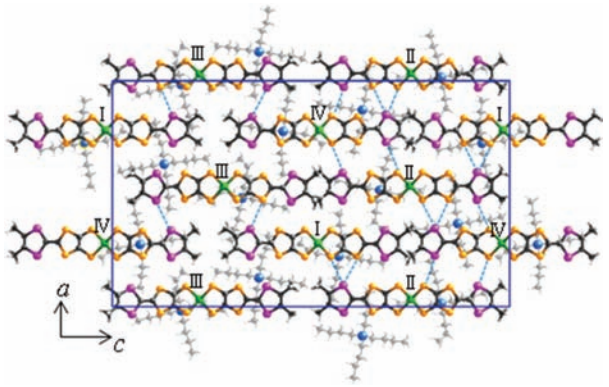

Figure 4. Arrangement of the Ni(dmstfdt)$_2$ anions at around $y \approx 0.125$ and the ^{n}Bu$_4$N cations at $y \approx 0.0$ in **3**. The dotted lines indicate short Se···Se and Se···S contacts less than the corresponding van der Waals distances.

crystallographically independent Ni(dmstfdt)$_2$ anions, **I**(**3**)–**IV**(**3**) (see Figure 4), are listed in Table 1. The average lengths of bonds *a*–*d* of **I**(**3**) and **II**(**3**) [2.169 (*a*), 1.716 (*b*), 1.368 (*c*), and 1.755 (*d*) Å] and those of **III**(**3**) and **IV**(**3**) [2.201 (*a*), 1.735 (*b*), 1.348 (*c*), 1.774 (*d*) Å], where the LUMO has a large amplitude (see Figure 2), are approximately equal to *a*–*d* of the monoanionic molecule [**C**(**1**)] and *a*–*d* of the dianionic molecule [**D**(**2**)], respectively. Thus, the charge distribution in **3** is not uniform but can be roughly represented as $\mathbf{I}^{-}\mathbf{II}^{-}\mathbf{III}^{2-}\mathbf{IV}^{2-}$. The semiconducting properties of **3** are thus ascribed to CO. The magnetic susceptibility (χ) of a polycrystalline sample of **3** showed Curie-like behavior at high temperature (χT = 0.379 emu K mol^{-1}). However, χ tended to decrease below about 6 K. These magnetic behaviors are consistent with the results of the structure analysis, suggesting the existence of a monoanionic Ni(dmstfdt)$_2^-$ molecule with $S = {}^1/_2$ spin. For clarification of the nature of the magnetic transition at around 6 K, further experiments are required.

In summary, the possibility of ICO in nickel complexes with selenium-containing extended-TTF dithiolate ligands was explored and discussed in terms of crystal structure analyses. Conventional CO was observed in **3**. However, whereas the fresh crystals of **1** were found to be Mott insulators, air oxidation of the crystal changed the electrical behavior to highly conducting. Moreover, **3** was found to exhibit a semiconducting CO state.

■ ASSOCIATED CONTENT

Ⓢ Supporting Information

Electromagnetic properties and structural data (CIF). This material is available free of charge via the Internet at http://pubs.acs.org.

■ AUTHOR INFORMATION

Corresponding Author

*E-mail: akoba@chs.nihon-u.ac.jp (A.K.), hayao@chs.nihon-u.ac.jp (H.K.).

Notes

The authors declare no competing financial interest.

■ ACKNOWLEDGMENTS

This work was financially supported by Grants-in-Aid for Scientific Research (B) (Grant 20350069), Young Scientists (B) (Grant 21750153), and Innovative Areas (Grant 20110003) from the Ministry of Education, Culture, Sports, Science and Technology of Japan. The study was also supported by the "Strategic Research Base Development" Program for Private Universities subsidized by MEXT (2009) (Grant S0901022).

■ REFERENCES

(1) Seo, H.; Hotta, C.; Fukuyama, H. *Chem. Rev.* **2004**, *104*, 5005.
(2) Sawano, F.; Terasaki, I.; Mori, H.; Mori, T.; Watanabe, M.; Ikeda, N.; Nogami, Y.; Noda, Y. *Nature* **2005**, *437*, 522.
(3) Seo, H.; Ishibashi, S.; Okano, Y.; Kobayashi, H.; Kobayashi, A.; Fukuyama, H.; Terakura, K. *J. Phys. Soc. Jpn.* **2008**, *77*, 023714.
(4) Ishibashi, S.; Tanaka, K.; Kohyama, M.; Tokumoto, M.; Kobayashi, A.; Kobayashi, H.; Terakura, K. *J. Phys. Soc. Jpn.* **2005**, *74*, 843.
(5) (a) Kobayashi, A.; Fujiwara, E.; Kobayashi, H. *Chem. Rev.* **2004**, *104*, 5243. (b) Kobayashi, A.; Tanaka, H.; Kobayashi, H. *J. Mater. Chem.* **2001**, *11*, 2078.
(6) (a) Suzuki, W.; Fujiwara, E.; Kobayashi, A.; Fujishiro, Y.; Nishibori, E.; Takata, M.; Sakata, M.; Fujiwara, H.; Kobayashi, H. *J. Am. Chem. Soc.* **2003**, *125*, 1486. (b) Zhou, B.; Shimamura, M.; Fujiwara, E.; Kobayashi, A.; Higashi, T.; Nishibori, E.; Sakata, M.; Cui, H.; Takahashi, K.; Kobayashi, H. *J. Am. Chem. Soc.* **2006**, *128*, 3872.
(7) Tsuchiizu, M.; Omori, Y.; Suzumura, Y.; Bobert, M.-L.; Ishibashi, S.; Seo, H. *J. Phys. Soc. Jpn.* **2011**, *80*, 013703.
(8) Mori, T. *Chem. Rev.* **2004**, *104*, 4947.
(9) Fujiwara, E.; Yamamoto, K.; Shimamura, M.; Zhou, B.; Kobayashi, A.; Takahashi, K.; Okano, Y.; Cui, H.; Kobayashi, H. *Chem. Mater.* **2007**, *19*, 553.
(10) Crystallographic data for **3**: orthorhombic, space group *Pbca*, *a* = 26.238(4) Å, *b* = 34.202(5) Å, *c* = 46.196(7) Å, *V* = 41456(11) Å^3 at 293 K, *Z* = 16. The final *R* factor was 0.083. Crystallographic data for **2**: triclinic, space group $P\bar{1}$, *a* = 13.294(5) Å, *b* = 13.984(6) Å, *c* = 18.332(8) Å, α = 111.146(4)°, β = 108.170(4)°, γ = 90.953(5)°, *V* = 2988(2) Å^3 at 293 K, *Z* = 2. The final *R* factor was 0.070. The crystal structure of **1** was previously reported.[9] However, the crystal structure was reexamined to obtain more accurate bond lengths, which were used in this paper. The lattice constants are *a* = 8.6884(3) Å, *b* = 19.6036(8) Å, *c* = 26.6969(11) Å, α = 110.559(2)°, β = 90.664(3)°, γ = 92.651(3)°, *V* = 4251.1(5) Å^3 at 293 K, *Z* = 4. The final *R* factor was 0.046.
(11) Non-spin-polarized MO calculations were performed at the density functional theory level with DMol^3 codes (Accelrys Inc., San Diego, CA).